University of BRISTOL

DEPARTMENT OF PHYSICS

FINAL YEAR PROJECT, DISSERTATION OR PHYSICS EDUCATION REPORT

NAME:	Rhys Alfred Shaw
DEGREE COURSE:	Bsc Physics with astrophysics
PROJECT TITLE:	Comparitive Study Between Sunyaev-Zel'Dovich and X-ray Selected Galaxy Clusters
YEAR OF SUBMISSION:	2020
SUPERVISOR:	Dr Ben Maughan
NUMBER OF WORDS:	6143

1 Declaration

The data collected in this project was collected equally by myself and my partner. Any data from the literature is referenced. We jointly contributed to the code that automated the CIAO analysis procesedure. I suggested the analysis of morphology as a measurement of axial symmetry and wrote the program to calculate it and approxiamte its error. Throughout the project we recieved help from our supervisor, Dr Ben Maughan. He helped us to get started with the analysis techniques and to introduce the topics important for this project. This took place with weekly meetings to check progress and have discussions of ideas relavent to the project.

1.1 Impact of Industrial Action

Industrial action only affected the cancellation of a few previously organised meetings and delays in responce to email queries.

1.2 Impact COVID-19

COVID-19 and the early closure of the university made us unable to access university for final weeks of the term. It also ment that some meetings where delivered online rather than in person.

CONTENT

page number

MNRAS **000**, 000–000 (0000) Preprint 6 May 2020 Compiled using MNRAS LATEX style file v3.0

Comparitive Study Between Sunyaev-Zel'Dovich and X-ray Selected Galaxy Clusters

Rhys Alfred Shaw
H. H. Wills Physics Laboratory, University of Bristol, Tyndall Ave, Bristol BS8 1TL, UK.

6 May 2020

ABSTRACT
This study investigates X-ray properties between X-ray selected galaxy clusters from the ROSAT PSPC All-sky survey and 400d survey and SZ selected clusters from the 2500-sqr degree SPT SZ survey. The cluster samples are observed with the Chandra X-ray observatory. The SZ sample consists of 17 cluster while the X-ray sample consists of 18 with redshifts of $0.35 \leq z \leq 0.9$ and $0.34 \leq z \leq 1.132$ respectfully. The study looks at the morphological types and L-T X-ray scaling relation of the samples. Morphologies are measured using a program that calculated the axial symmetry of the clusters around the peak emission. This study finds that there is no significant difference in the morphological distribution of the samples, and finds that there is no significant systematic difference in the L-T scaling relations.

1 INTRODUCTION

1.1 Background

In the very early universe, tiny fluctuations in density caused the collapse of matter into dark matter dominated structures called galaxy clusters. These are the largest structures known to exist and, due to their large mass, make very good candidates to probe cosmology. This is because the mass function is sensitive to the expansion history and structure of the universe. Understanding the mass function is critical to understanding the cosmological parameters underpinning the universe (Kravtsov & Borgani 2012). Galaxy clusters were found to contain large amounts of unseen matter. Zwicky (1937) found that in the Coma cluster, its viral mass was more than what was observable from constituent galaxies. Leading to only one consequence; most of the cluster's mass did not interact with light.

Clusters are now known to be comprised of $\approx 90\%$ dark matter, 9% hot gas known as Intracluster medium (ICM), and 1% galaxies. Clusters were formed as a result of variations in the density of the early universe. The denser regions collapsed into a large gravitational potential. Baryons falling into this potential well gained kinetic energy and, due to shocks with baryons within the centre of the potential, were heated to high temperatures $\approx 10^8 K$ (Giodini et al. 2013). These temperatures are high enough for the of emission X-ray photons via the process of thermal bremsstrahlung. As the emission of X-rays is deeply connected to the mass of the cluster, this mechanism provides access to the underlying structure of the cluster. The temperature of clusters is mildly affected by feedback from galactic processes such as AGN and Supernovae. These effects are usually minimal, and their impact can be tested through hydrodynamical simulations.

Galaxy clusters were initially observed through telescopes in the optical regime, and Abell (1958) first published a catalogue of these clusters. These clusters were rich in galaxy content and were identified as clusters for that reason. These early surveys looked for rich groups of upwards of 1000 galaxies gravitationally bound. The X-ray emission from a clusters ICM presents an alternate way of surveying galaxy clusters, rather than looking for galaxy groupings the sky can be surveyed for X-ray emission and clusters can be found from this. It is easier to look for extended X-ray sources than it is to look for galaxies bound by gravity. X-ray samples are chosen from X-ray surveys with a minimum flux limit to select an appropriate sample size. X-ray observations can be used to measure and calibrate a mass function of galaxy clusters.

Clusters are not limited to detection in these ways. Another effect that can be used to survey clusters is the Sunyaev-Zel'Dovich (SZ) effect. This is the process of CMB photons inverse-Compton scatting with high energy electrons within the ICM. A CMB photon has about a 1% chance of scattering with a high energy electron and will create a signal that stands out from the CMB. For a detailed study of this effect see Birkinshaw (1999), for original work see Sunyaev (1970) and Sunyaev & Zeldovich (1972). The result of this effect leads to a microwave signature that can be detected with telescopes, such as the south pole telescope (SPT). SZ surveys were conducted first by the PLANCK microwave observatory creating a new way to choose galaxy cluster samples. SZ selected clusters did not have to consider selection effects that are commonly associated with X-ray flux-limited samples as their X-ray analysis was done independently of their detection and selection criteria. This presents the advantage of selecting clusters from SZ surveys as opposed to an X-ray flux limited sample. At present, the South Pole Telescope conducted the most recent SZ survey covering 2500-sqr degrees.

Selection effects have been known to exist in astronomy for a long time and have noticeable effects on the analysis of data from these samples. A selection effect or bias is where the way an object is selected creates systematic bias within any analysis done on the object. The impact of this effect will depend of the type of analysis that is conducted, and it can be significant enough to create incorrect interpretations of data. Understanding selection bias is critical especially when looking for accurate mass proxy for use testing cosmological parameters. Some effects are expected to be present in results for flux-limited samples such as the Malmquist effect, where the survey sample is limited by the fact that low luminosity clusters will not be detected to the same redshift as higher luminosity clusters. Leading to an effect where only high luminosity clusters are seen at large redshift (Gould 1993). This effect is not present within SZ selected samples and consequently are preferable to an X-ray sample for high redshift studies (Andersson et al. 2011).

The physical observables of a cluster have been shown to follow scaling relations and were first proven mathematically by Kaiser (1986). Well calibrated X-ray scaling relations allow for simple calculations of galaxy cluster mass and luminosity from only ICM temperature measurements of galaxy clusters. It is well known that redshift, flux and ICM temperature of a galaxy cluster do not require any assumptions about cosmology to be measured. Flux and redshift can be used to determine the luminosity distance of a cluster, relating these properties to cosmological parameters, to calculate luminosity. Some studies have used cluster scaling relations to test the isotropy of the Hubble expansion (Migkas & Reiprich 2018). Cluster scaling relations have been well studied (Vikhlinin et al. (2002), Ikebe et al. (2002), Ettori et al. (2003), Short et al. (2010)), particularly the X-ray luminosity-ICM temperature scaling relation.

The dynamics of clusters ICM can be studied, provided high-resolution X-ray imaging. The X-ray emission from the ICM creates a projection of the three-dimensional clusters morphology. The morphological properties of cluster allow for various astrophysical features to be studied, such as cooling flows (Vikhlinin et al. 2007). Clusters are occasionally found as merger systems, where two or more clusters are pulled together into a larger system leading to a disturbed morphology.

1.2 Theory

Galaxy clusters have multiple observables that have been shown to scale well with the size of the cluster such as X-ray luminosity temperature, morphology and the intensity of the Sunyaev Zel'Dovich effect. The theory of self-similarity between clusters, meaning that clusters are scaled versions of each other, leads to the idea of scaling relations between cluster properties. These can be used to relate cluster mass to more measurable quantities like temperature and luminosity. X-ray observations are widely used to analyse cluster characteristics due to the Chandra and XMM-newton satellites measuring high quality data from high redshift clusters. Self-similar clusters will have simple power-law relationships between the X-ray properties of the ICM. Assuming that the heating of the ICM is only done by the gravitational potential, then the relations between ICM temperature (T_{ICM}) and X-ray luminosity (L_X) is expressed as:

$$L_X \propto E(z) T_{ICM}^2, \tag{1}$$

where E(z) describes the redshift evolution of the Hubble parameter and is expressed below.

$$E(z) = \frac{H_z}{H_0} = [\Omega_m (1+z)^3 + (1-\Omega_m - \Omega_\Lambda)(1+z)^2 + \Omega_\Lambda]^{\frac{1}{2}}. \tag{2}$$

A relationship between the cluster's mass and temperature of the ICM can be derived by assuming that the ICM is in hydrostatic equilibrium, that the pressure gradient of the gas is balanced with the gravitational force. This leads to the relation between cluster mass and ICM temperature:

$$M_{\Delta_z} \propto T_{ICM}^{\frac{3}{2}}, \tag{3}$$

Where M_{Δ_z} is the mass within a sphere of radius $R_{\Delta z}$, the radius where the density within the sphere is an integer (Δz) multiple of the critical density of the universe $\rho_c(z)$. This over-density radius is necessary to distinguish an edge of the cluster. For a more detailed derivation of scaling relations see Giodini et al. (2013).

Galaxy clusters are not always seen as radially decaying spherical distributions of matter, despite what the self-similar assumption assumes. These variations come from events like formation and cluster mergers. Consequently, clusters are seen to be in many shapes, usually categorised into Relaxed and unrelaxed clusters. Understanding the Morphology type of clusters can give information on the dominant physical processes within clusters, their formation histories and potentially give insight into the large-scale evolution of the universe.

This study will compare X-ray properties of two samples of galaxy clusters. A X-ray selected sample from the ROSAT PSPC All-sky and 400d surveys and a SZ effect selected sample from the 2500-sqr degree SPT SZ survey. The samples have had follow up X-ray observations made with the Chandra observatory. It will calculate the L-T scaling relations for both samples and model the relations with a linear regression algorithm. An axial symmetry morphology will be calculated for each galaxy cluster and their distributions analysed with a Kolmogorov-Smirnov test. The samples will receive the same data reduction and analysis process to ensure any difference in the procedure is not interpreted as a systematic selection effect. This work uses the ΛCDM cosmological model throughout with, $H_0 = 70 kms^{-1} Mpc^{-1}$, $\Omega_m = 0.3$ and $\Omega_\Lambda = 0.7$.

This work is organised as follows. Section 2 describes the cluster samples for both SZ and X-ray observations. Section 3 discusses the analysis steps that the clusters went through, including how the Chandra data was processed and how the mass was estimated, along with the spectral analysis and morphological analysis. Section 4 discusses the results of the analysis, along with how the data was modelled. Section 5 contains a discussion of morphology and the L-T scaling relation. Finally, Section 6 concludes with a summary of the contents of this work.

2 SAMPLES

The two cluster samples described below are from an X-ray survey and SZ survey respectfully. There were some criteria required for the samples. Firstly, it was ideal to have similar size samples with similar redshift ranges to ensure a fair comparison. Secondly, as this study is only analysing Chandra data, the clusters needed to have Chandra observations.

- The X-ray sample was selected from the ROSAT PSPC All-sky and 400d surveys. This sample is a selection of clusters from a previous sample used and first collected by Vikhlinin et al. (2009) (V09). The sample contains 18 clusters with a requirement that the ROSAT derived flux was no lower than 2.2×10^{-13} cgs . The sample has a redshift range of $0.35 \leq z \leq 0.9$. The sample was originally 20 cluster, but due to a problem finding the observational data for clusters CL1524+0957 and CL1226+3332 they were taken out of the final sample.
- The SZ sample contains 17 clusters that were selected from the 2500-sqr degree SPT SZ survey (Bleem et al. 2015). This is a sample with signal-to-noise ratio > 12.5 and a redshift range of $0.34 \leq z \leq 1.132$. This sample had many clusters excluded due to the availability of Chandra observational data.

3 DATA PROCESSING AND ANALYSIS METHODS

3.1 Chandra Processing

The data presented in this work went through the following processing steps below, using CIAO software version 4.11 and CALDB, calibration database, version 4.8.5. This ensures that each cluster received consistent calibration. The data used in this work were detected on the ACIS-I chip of the Chandra X-ray observatory. The chip was in VFAINT mode for all of the observations. This was important as it helps to distinguish between good X-ray photon detections and those that are likely to be from cosmic rays.

- The raw events files were reprocessed with the *Chandra_repro* task, in which bad-pixels and afterglows from cosmic ray events are corrected. The latest calibration is applied in order to update quantities such as coordinates, time and status information of the events.

- The events file then required cleaning to look for any anomalous background rates, such as solar flares in the ACIS observations, and removed from the events file. This was done by creating a light curve with the CIAO tool *lc_clean* algorithm where a visual inspection was done.

- The events file was checked for any point sources using the CIAO algorithm *wavdetect*. These were inspected before being excluded from the data. Any false detections were removed if necessary.

- Cluster emission was analysed with radial profiles to find the extent of emission. This was done by creating $\approx$ 40 annuli around the cluster, centred on the peak emission. The flux in each annulus is calculated. By looking at the radial profile of a clusters emission, the first approximation to the boundary of the clusters can be made. Background regions for the cluster where also made here.

- To create a spectrum, the algorithm *specextract* was used to create weighted RMFs and ARFs for the source and background regions. Exposure corrected images were created to account for the inconsistencies in sensitivity across the CCD. These corrected images were then used to detect sources in the data. The regions calculated where checked by eye and removed from the image after appropriate alterations where necessary. These steps resulted in the data being calibrated, cleaned, and sources removed before spectral analysis.

3.2 Spectral Analysis

As bremsstrahlung emission has a characteristic continuous spectrum, temperature and energy flux of the data can be determined through an analysis of its spectrum. The background regions for this analysis were created individually for each cluster from the same image. As determining the background region will depend somewhat on human intervention, it was necessary to create some guidelines to ensure consistency where possible. First, a radial profile was made, as discussed in Section 3.1. This was used to determine the minimum distance this region is required to be to ensure no interference by the out regions of the cluster. The background regions also required to be of similar exposure to the cluster to minimise possible variation from the true background level. The spectra for each cluster was extracted from within the required radius and was fitted using the APEC model. This will model the spectrum to the emission from thermal bremsstrahlung with traces of metal emission lines. In addition, the TBABS model was used to account for ISM grain absorption along the line of sight to the cluster. The fitting statistic used throughout was the Poisson WSTAT statistic. The data closely resembles a Poisson distribution so is not suited to a chi-squared fitting procedure.

Model parameters of hydrogen column density were found using the COLDEN program, which contains the library of Dickey & Lockman (1990), and fixed. Redshift was fixed to the value available in the literature. The model gives values of ICM temperature, X-ray luminosity and relative metallic abundance, the latter of which was not used for any comparative test as the X-ray samples quality proved insufficient to meaningfully constrain this. The luminosity was calculated across the entire energy range to calculate the bolometric luminosity of the cluster.

To consistently use an appropriate radius for each cluster, it was necessary to calculate the mass of the cluster. The cluster mass M_{500} of both samples were calculated from the M-T scaling relation calculated from V09. This relationship is described below:

$$M_{500} = M_0 (T/5keV)^{\alpha} E(z)^{-1}, \quad (4)$$

where $M_0 = (3.02 \pm 0.11) \times 10^{14} h^{-1} M_{\odot}$ and $\alpha = 1.53 \pm 0.08$. This relation was selected due to its consistency with the self-similar expectation. Arnaud et al. (2005) also formulated a similar relationship. By calculating the temperature of an initial region. R_{500} can be determined from equa-

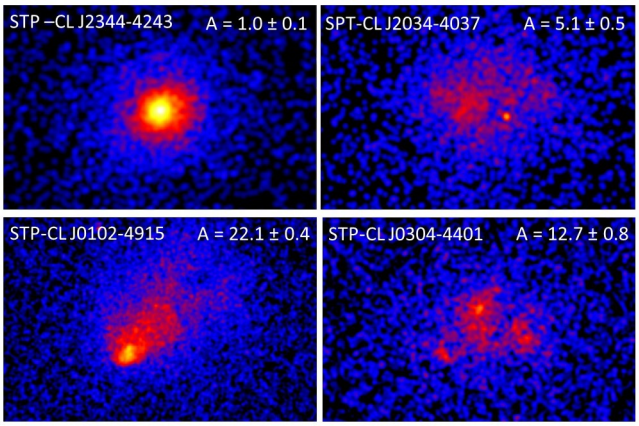

Figure 1. Morphology Axial symmetry values for a small selection of the SZ sample. These images have been smoothed as a visual aid of the cluster structure. The four clusters show the range of axial symmetry.

tion (4).

$$R_{500} = \left(\frac{3M_{500}}{4\pi 500\rho_c(z)}\right)^{1/3} h^{-1/3}, \quad (5)$$

where $\rho_c(z) = \frac{3H_z^2}{8\pi G}$. This process was initially iterated until convergence, which was found to converge with sufficient uncertainty after only one iteration due to limited temperature dependency on radius. The radius used for the analysis was first at R_{500}, however as some clusters failed to model the temperature to sufficient uncertainty at this radius. The radius was reduced to $0.5R_{500}$ to ensure a consistent measurement was used for both samples.

3.3 Morphology Analysis

This work also aims to look for any differences in morphology between the two samples. To do this quantifying the morphology of galaxy clusters was an important step to ensure an accurate interpretation. Morphologies are easy to classify as mergers or non-mergers, and relaxed/unrelaxed. However, creating a quantitative approach to categorising Morphology comes with many positives, such as allowing for statistical tests. An ideal relaxed galaxy cluster would be perfectly axial symmetric, a measure of this symmetry would be an approach to quantify the distribution of the cluster. To calculate this morphological statistic, a region around the cluster from the processed and cleaned level 2 events file was required, which needed to be centred on the cluster. Axial symmetry, $A = |\vec{a}|$, was then calculated by evaluating each pixel by its flux value and displacement vector (the distance that pixel is from the central region).

$$\vec{a} = \frac{1}{< f_n > N} \sum_n^N f_n \vec{D_n}, \quad (6)$$

where n is the pixel number, N represents the total number of pixels. $\vec{D_n}$ is the displacement vector of pixel n and f_n is the photon flux of the pixel. It can be seen from equation (5) that a pixel with $\vec{D_n} = 5\vec{i} + 5\vec{j}$ will be weighed more than a pixel with $\vec{D_n} = 2\vec{i} + 2\vec{j}$ as the distance from centre is greater. This will result in a cluster with a symmetric high flux distribution around the centre, but with a very asymmetric distribution of lower flux having a larger overall A. This resulted in cluster asymmetry in the outer region being an important contribution to the overall statistic. A is partially independent of the background as an isotropic distribution has very high axial symmetry so consequently will not affect the statistic. However, for a large region, any variation in background symmetry around the outer edge will adversely affect the statistic. This highlights the importance of selecting as small a region as possible around any cluster, whitest still encompassing the clusters features. This approach to qunatifying morphology is similar to work previously done by Nurgaliev et al. (2013) (N13). The main difference in N13s method is that instead of calculating the statistic as a sum of vectors, the axial symmetry was calculated for annuli around the cluster and then averaged to form the final statistic. N13 showed that the measuring axial symmetry agrees well with centroid shift, a more common method of quantifying morphology.

A was calculated using a python program that read the observational data. When the program was first made it was tested by inputting known perfectly axial symmetric distributions (square boarder) and progressed to mock cluster data. This was to ensure the calculation was made correctly and simple expected relationships where seen. The errors for this statistic were approximated using Monte Carlo methods. This consisted of creating 10,000 new images of each cluster. The flux value of each new pixel was taken randomly from a Poisson distribution with mean of the original pixels flux. The statistic was calculated from these new images and the mean and standard deviation was determined.

Table 1. SZ selected cluster sample properties from within a radius $0.5R_{500}$.Column (2): redshift of the cluster. Column(3): temperature of the clusters ICM. Column(4): Bolometric lumoinsity of the cluster. Column(5): Axial symmetry of the cluster around the peak of emission.

Cluster Name	z	T keV	$L_{X,Bol}$ 10^{45} $erg\ s^{-1}$	A
SPT CLJ2248−4431	0.350	10.0±0.7	6.99±0.13	$10.1^{+0.2}_{-0.2}$
SPT CLJ0102−4915	0.870	15.1 ±1.5	13.40±0.26	$22.1^{+0.4}_{-0.4}$
SPT CLJ2344−4243	0.596	14.3±1.0	11.60±0.29	$1.0^{+0.1}_{-0.1}$
SPT CLJ0438−5419	0.421	13.1±1.4	3.17±0.09	$4.6^{+0.4}_{-0.4}$
SPT CLJ2106−5844	1.132	10.5±2.2	5.91±0.34	$2.1^{+0.7}_{-0.5}$
SPT CLJ2337−5942	0.775	7.2±1.8	3.32±0.15	$2.3^{+0.6}_{-0.4}$
SPT CLJ0040−4407	0.350	6.9±0.7	1.45±0.07	$1.0^{+0.7}_{-0.3}$
SPT CLJ2031−4037	0.342	8.5±1.1	2.22±0.07	$5.1^{+0.5}_{-0.5}$
SPT CLJ0304−4401	0.458	6.4±3.6	0.72±0.06	$12.7^{+0.8}_{-0.8}$
SPT CLJ0411−4819	0.424	9.0±2.6	1.69±0.14	$11.5^{+1.0}_{-0.9}$
SPT CLJ0234−5831	0.415	7.0±1.0	1.83±0.07	$6.0^{+1.0}_{-0.9}$
SPT CLJ0417−4748	0.581	5.8±0.5	2.37±0.08	$1.6^{+0.3}_{-0.3}$
SPT CLJ0304−4921	0.392	6.5±0.6	1.18±0.06	$1.7^{+0.5}_{-0.4}$
SPT CLJ0555−6406	0.345	11.5±3.9	1.33±0.09	$9.2^{+1.1}_{-1.0}$
SPT CLJ2145−5644	0.480	7.4±1.2	1.20±0.06	$1.3^{+0.7}_{-0.4}$
SPT CLJ2325−4111	0.358	11.8±3.2	1.21±0.04	$6.0^{+0.9}_{-0.9}$
SPT CLJ2341−5119	1.003	9.3±2.6	2.41±0.01	$1.8^{+0.4}_{-0.3}$

Table 2. X-ray selected cluster sample properties from within a radius $0.5R_{500}$.Column (2): redshift of the cluster. Column(3): temperature of the clusters ICM. Column(4) Bolometric lumoinsity of the cluster. Column(5): Axial symmetry of the cluster around the peak of emission.

Cluster Name	z	T keV	$L_{X,Bol}$ $10^{44}\ erg\ s^{-1}$	A
CL 0302−0423	0.350	4.5±0.2	15.1±0.59	$0.2^{+0.5}_{-0.0}$
CL 1212+2733	0.353	7.6±0.9	9.75±0.26	$4.8^{+0.8}_{-0.7}$
CL 0809+2811	0.399	5.9±1.0	6.38±0.30	$7.3^{+0.8}_{-0.7}$
CL 0318−0302	0.370	4.8±0.6	4.76±0.26	$8.6^{+0.8}_{-0.7}$
CL 1416+4446	0.400	4.6±1.7	4.10±0.35	$3.1^{+0.6}_{-0.5}$
CL 1701+6414	0.453	3.2±0.8	5.24±0.21	$2.6^{+0.4}_{-0.4}$
CL 1003+3253	0.416	4.1±0.4	3.79±0.26	$3.1^{+0.4}_{-0.4}$
CL 0159+0030	0.386	6.4±0.9	4.04±0.26	$0.1^{+0.6}_{-0.1}$
CL 0141−3034	0.442	2.7±0.7	0.92±0.16	$1.9^{+1.1}_{-0.6}$
CL 1120+4318	0.600	5.0±0.7	9.89±0.52	$5.9^{+0.8}_{-0.7}$
CL 1641+4001	0.464	5.3±1.0	2.61±0.23	$1.6^{+0.6}_{-0.4}$
CL 0350−3801	0.363	3.4±0.4	1.26±0.28	$1.0^{+1.1}_{-0.3}$
CL 0355−3741	0.473	5.2±1.1	4.40±0.25	$2.6^{+0.7}_{-0.5}$
CL 0958+4702	0.390	4.0±0.4	2.05±0.27	$1.1^{+0.5}_{-0.3}$
CL 1312+39(00)	0.404	4.2±0.8	2.25±0.53	$4.7^{+0.8}_{-0.7}$
CL 0333−2456	0.475	4.8±1.7	2.19±0.24	$4.3^{+0.8}_{-0.7}$
CL 0030+2618	0.500	6.4±2.1	4.23±0.33	$2.0^{+1.2}_{-0.6}$
CL 0230+1836	0.799	7.7±1.4	6.14±0.28	$5.7^{+0.6}_{-0.6}$

4 RESULTS

4.1 Modelling the $L-T$ Relation

The results from the L-T relation of the two samples are presented and briefly discussed. Table 1 and Table 2 contain the data for each cluster used in this work for the SZ and X-ray samples respectfully. The scaling relation was fitted to the samples using the program LINMIX, which uses a Bayesian method to account for errors in linear regression, as discussed in Kelly (2007). The fit of the data will take the form of equation (1) and was fitted in log space against T.

$$\frac{L_{X,Bol}}{E(z)} = 10^{\alpha}\left(\frac{T}{T^{*}}\right)^{\beta}(ergs^{-1}), \tag{7}$$

where α and β are fit parameters calculated from LINMIX. Fig.2 shows the form of the L-T scaling relation of the two samples. Following convention T is in units of energy and is fully represented by kT, this is used throughout this work. T^{*} set to 5 keV for the X-ray galaxy clusters sample and 8 keV for the S-Z sample. These were chosen as the approximate median temperature of the respective galaxy clusters samples. The measured parameters of these fits are shown in Table 3.

With a brief look at the fitting parameters of both samples there is a significant agreement in the β parameter. It can also be seen that the normalisation, α, are not so in agreement. However, Maughan et al. (2012) suggests that scatter in the normalisation is expected to be dependent on the dynamical state of the cluster and its morphological type. This could be a result of a difference in the morphological distributions of the two clusters samples resulting in a scatter in L. The intrinsic scatter of the X-ray and SZ samples are similar, with the X-ray sample having a large error which makes it difficult to judge how much they agree. As the parameters are in good agreement it was decided to combine the sample to look at how the parameters would change with a larger sample of 35 clusters. The two samples cover a different range in temperature, so combining them will allow for a greater range to be modelled. The combined parameters seem to vary further from the expected $\beta = 2$, from the self-similar relationship, and has resulted in an increased normalization. The combined L-T scaling relation has a slightly smaller intrinsic scatter and error. This is expected as clusters that contribute to the intrinsic scatter the most will not be weighted as much within the larger sample. Low scatter is consistent with the presence of slowly cooling centre core regions. If the samples were abundant in cold core regions (CC) then it would result is a scatter in L. This is discussed further in Section 5.2.2.

Table 3. Fitting parameters of the L-T scaling relation for different samples, σ indicates the intrinsic scatter around the regression line.

Sample Name	α	β	σ
X-ray	44.6 ± 0.1	2.3 ± 1.1	0.08 ± 0.4
S-Z	44.16 ± 0.08	2.3 ± 0.8	0.08 ± 0.04
Combined	44.82 ± 0.05	2.5 ± 0.3	0.07 ± 0.02

4.2 Morphological Distribution

In this section, the distribution of axial symmetry is presented and briefly discussed, as well as a comparison to axial symmetry calculations from a past study. The morphological distributions of the cluster samples are shown in Fig. 4 as a histogram. The two-sample Kolmogorov-Smirnov (KS) test of empirical distributions was used. The statistic was used to create a p-value of the null hypothesis, that these two distributions come from the same model distribution. The p-value was calculated to be $p = 0.35$. This statistical test is sensitive to the shape of the distribution functions and any differences in the location.

Mergers of galaxy clusters will create an increase in axial symmetry, A. We can define a minimum A for which the clusters are likely to be a merger. Referring to Fig. 1, we can see that SPT-CL J0102-4915 and SPT-CL J0304-4401 (the two bottom clusters) seem likely to be ongoing mergers. From looking at the full sample of clusters, we can assign a value A for which clusters can be categorised as a merger. This was found to be $A > 7$. The determination of this value was conducted with a visual analysis of the clusters and so was sensitive to the S/N ratio of the source as the appearance of structure would be difficult to determine. It is known that merging systems that are along the line-of-sight will not be detected as mergers as the asymmetry of the cluster will be impossible to see in a 2D statistic. However, as this requires a specific orientation it is likely to have only a small impact on the distribution of a large sample.

Comparing this morphology metric to different work allows for its validity to be tested. Nurgaliev et al. (2017)(N17) presented work where a morphology metric was calculated for X-ray and SZ selected galaxy clusters. Fig 5 presents N17s values compared to the calculated axial symmetry. The figure shows a positive correlation between the two metrics,

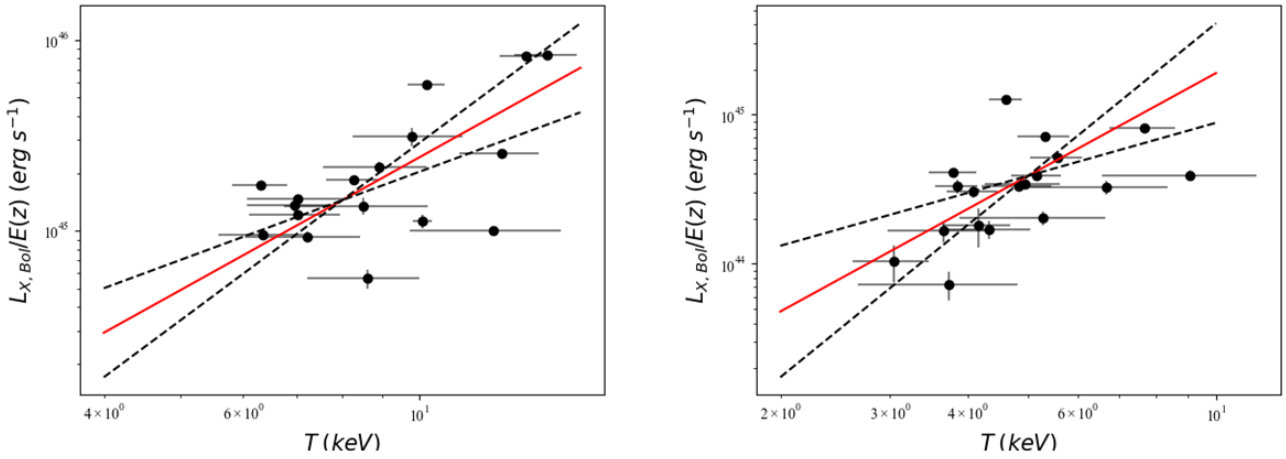

Figure 2. Top left: L-T scaling relation of SZ selected clusters from the 2500sq deg SPT SZ survey. Top right: L-T scaling relation of X-ray selected sample from the ROSAT PSPC All-sky and 400d survey. The Redline indicated the best-fit to data and the dashed lines indicate the range of gradient error.

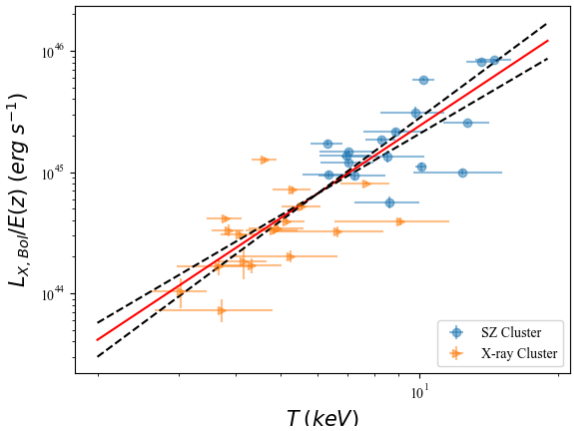

Figure 3. L-T scaling relation for a combined sample of X-ray selected galaxy clusters, from the ROSAT PSPC All-sky and 400d surveys, and SZ selected galaxy clusters from the 2500sq deg SPT SZ survey. The Redline indicated the best-fit to the data and the dashlines indicate the range of error on the parameter β.

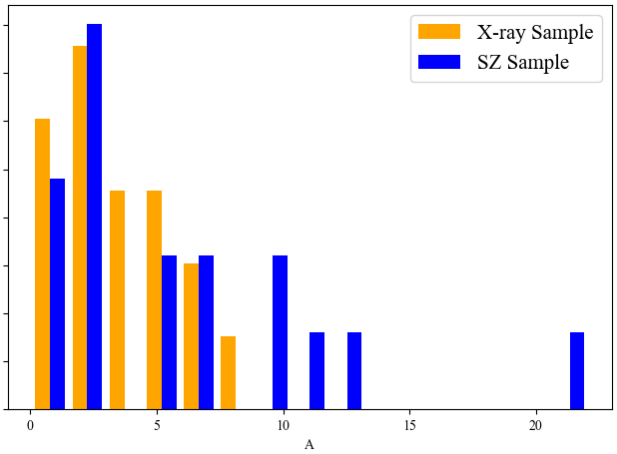

Figure 4. Distribution of axial symmetry statistic form X-ray clusters selected from the ROSAT PSPC All-sky and 400d surveys, and SZ clusters from the 2500sq deg SPT SZ survey. The KS test values for the distributions is 0.30 with a p-value $p = 0.35$.

whether this relationship is linear is not so clear. N17 also determined a value for which clusters would be classified as mergers and found a value of 0.6. The difference in these two values means that our clusters have more classified mergers than if measured using the method used in N17.

5 DISCUSSION

5.1 Morphological Comparison

In the past, it has been suggested that SZ selected galaxy clusters are often biased towards detecting morphologically disturbed clusters. This idea came as the earliest SZ clusters were found to be a very dynamic mergers, such as the "El Gordo" cluster (Menanteau et al. 2012). This led to the discussion of new merger clusters within the literature. It has also been suggested that the PLANCK observatory, which first detected galaxy clusters using the SZ effect, was more sensitive to merger systems (Rossetti et al. 2016). It is thought that SZ clusters are not inherently biased to merger systems. Fig 4 shows the morphology distributions of the two cluster samples. It can be said with certainty that the two distributions in this study are not different in any statistical sense. Consequently, the presence of a SZ bias towards more dynamic clusters is not supported. The p-value of the KS test was found to be $p = 0.35$. It is common to reject the null hypothesis of the KS test for $p \leq 0.05$, so we required this to say with statistical significance the two distributions are different.

The morphology statistic was calculated by considering the axial symmetry of each cluster. It has already been said that this value is dependent on the background for samples with a low signal-to-noise ratio and is sensitive to the size

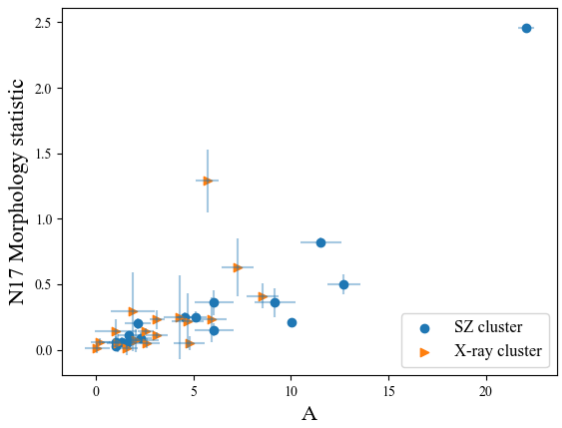

Figure 5. Axial symmetry of both SZ and X-ray galaxy cluster samples plotted against axial symmetry calculated by N17.

of the selected regions. Fig 5 shows how the morphology statistic used in this work compares to that used by N17. The two statistics generally agree with each other except for CL 0230+1836. This X-ray selected cluster was the faintest cluster with a high redshift of $z = 0.799$. Upon visual inspection of this cluster, it is apparent that the cluster should be classified as a merger, but due to its significantly low signal-to-noise ratio the statistic fails to calculate it accurately.

The axial symmetry statistic could be ideally calibrated though an analysis of simulated clusters with set morphological distributions. This would allow for an improved determination of what would be called a disturbed cluster. A greater understanding of the statistics dependency of on the S/N ratio can be better studied and allow for improvements in the statistic to account for this. Hydrodynamical simulations that model gas dynamics, star formation, supernovae feedback and AGN feedback will allow the statistic to be tested on their dependencies aswell. Ideally this dependency will be negligible. The orientation of a merging cluster will impact the 2D projection onto the detector. Simulations can be used to rotate a merging system, project that system onto a detector and calculate its axial symmetry. This will allow for a dependency on the clusters orientation to be determined. The results of this work show that there is insufficient evidence to suggest SZ clusters are more morphologically disturbed than X-ray selected clusters. It is more prevalent that the largest factor affecting this would be from the archival bias towards merger systems due to early interest in such systems.

5.2 L-T Comparison

5.2.1 Luminiosty Measurements

In this section, the luminosity measurements of both samples were compared to previous studies. Bulbul et al. (2019) (B19) calculated the bolometric luminosity of 60% of the clusters used in the SZ selected sample, unfortunately luminosity values of the others were not found. Figure 6 displays the luminosity calculated from the work above, compared to that calculated in this work. The SZ sample and B19 are bolometric luminosities. A line with gradient 1 was added to demonstrate that they are in good agreement. The single cluster that deviated furthest from the line is SPT-CLJ0304-4401. This is a particularly faint cluster. B19 used observational data from XMM-Newton, it is widely known that there are systematic errors that arise when comparing Chandra and XMM-Newton studies, however these effect cluster temperatures more than flux. The observation time of SPT-CLJ0304-4401 is only 15ks, which is lower than most observation used in this study. The exposure time of the XMM-Newton observation was likely to be different, which can affect the flux measurement of the cluster.

V09 calculated the luminosity of the X-ray selected clusters within the photon energy range (0.5–2)keV. The calculated luminosity in this work is bolometric luminosity, which will inevitably mean that there will be a deviation from perfect 1:1 agreement. The X-ray sample bolometric luminosities compared to V09 show good agreement with each other, except for cluster CL 0141-3034. This cluster is particularly faint, and a centre region is difficult to determine accurately. The variation could be a result of choosing a different centre of the cluster around which the luminosity was measured. Several things can cause differences in luminosity measurements. Radial size of luminosity measurement is not specified in V09. However, it is likely that this was within a region of radius R_{500}. This is compared to the $0.5R_{500}$ used in this study, leading to the possibility that there is the exclusion of the outer cluster regions, resulting in lower measurements of flux. The background selection method used in V09 is similar to the method used in this work and is unlikely to cause a significant difference. Therefore, it is likely that the luminosity measurement of CL 0141-3034 is an underestimate.

There are two ways in which the background of a sample is considered in X-ray observation. A simple way to approximate the background, used in this work, consists of choosing a region with the absence of extended and point sources. Another is extracting a background approximation from blank-sky files. These files have been produced from many Chandra observations and will give a tailored background spectrum to specific observations. These provide background files when extended sources are so large that a background region on the ACIS cannot be estimated from the data set. These background regions create spectra that are subtracted from the cluster region. Regions that vary from the true background will negatively affect the flux. This is demonstrating why it is important, in the analysis of galaxy cluster scaling relations, that the background is a good approximation of the true background.

5.2.2 Sources of Intrinsic Scatter

From Fig 3 and 4, it is easy to see the impact of scattering effects on the clusters. Table 1 shows that the intrinsic scatter (σ) within both samples is very similar. This scattering is thought to be caused by several things, the most important of which will be discussed here. The first source of scattering is related to the dynamical state of the cluster and hence its morphological type, which was briefly mentioned previously. Clusters that are in a relaxed state are likely to have what is commonly called cold core (CC) regions. This is when the central region of the cluster cools from emission and consequently becomes dense, which in

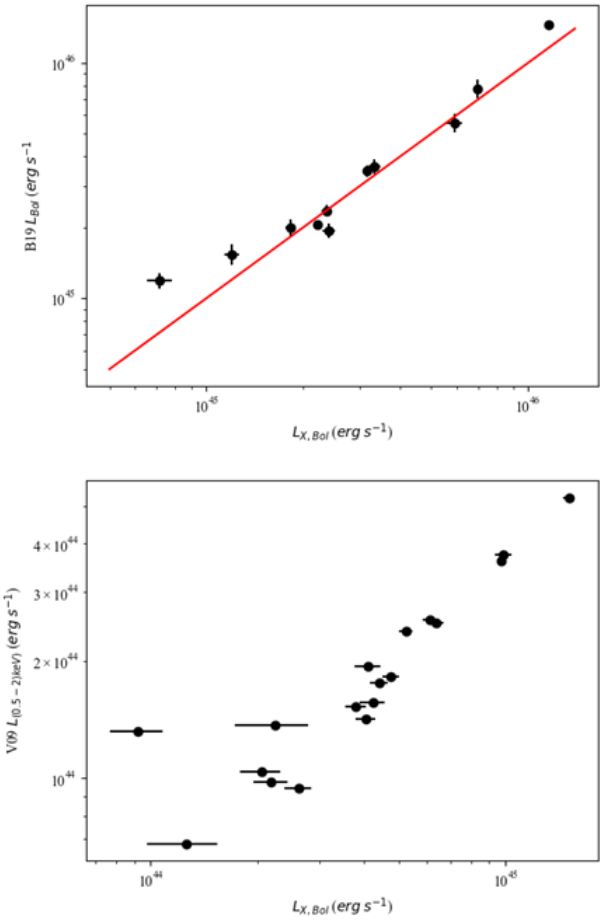

Figure 6. Top: $L_{X,Bol}$ calculcated for the SZ sample of galaxy clusters selcted from the 2500sq deg SPT SZ survey. Plotted with L_{Bol} from (B19). Bottom: $L_{X,Bol}$ calculated for the X-ray sample selected from the ROSAT PSPC All-sky and 400d-surveys. Plotted with the $L_{(0.5-2)keV}$ from V09.

turn creates higher emission. Causing clusters to be observing higher luminosities for a given temperature, scatting in L. The cumulative effect of which will change the slope of the L-T relation, and with an abundance of CC in a sample will increase the normalization. This could be partly responsible for the difference in the fit parameters that we see. If we consider this when looking at the X-ray and SZ fit parameters shown in Table 1, we can see that the X-ray sample has a larger normalisation than what is seen in the SZ sample.

Intrinsic scatter is also impacted by the morphological distributions of the samples. Scaling relations assume that the ICM is spherically symmetric, but it is known that clusters are triaxial structures with varying morphologies. Buote & Humphrey (2012) found that this effect can introduce a scatter of $\approx 10\%$ in the SZ Compton parameter (y). Effecting the S/N ratio of SZ selected clusters. It also suggests a small scatter in the ICM temperature. Understanding the shape of the ICM is key to for a determination of mass that is unbiased. The results from Fig 4 show that there are marginally more merger systems within the SZ sample than X-ray, creating reason for there to be a variation in their fitting parameters. A method of accounting for morphological effects comes from Limousin et al. (2012)(L12), where a multi-wavelength observation of the ICM is used to account for the triaxial nature of the ICM.

The source of scattering that seems to be overlooked in X-ray scaling relations is from possible anisotropy of the Hubble expansion in the universe. Migkas et al. (2020) (M20) most recently studied this anisotropy. This study tested the isotropy of the universe using the L-T relation as a probe. The study looked galaxy clusters from across the galactic sky and found significant anisotropy across the universe. This is not the only study to find this type of anisotropy as consistent results have been found from (Webb et al. (2011), Feindt et al. (2013), Kalus et al. (2013),Bengaly et al. (2017)). M20 suggests that either the known cosmology of the universe requires some adjusting, or there is an unknown bias effect that needs to be accounted for. Whatever the true reason for this result galaxy cluster scaling relations seem to be affected by this anisotropy. The effect of which will be that the luminosity of clusters will be scattered. If the effect is modelled effectively, the galactic position of the cluster can be used to estimate this scatter and appropriately account for it. This type of intrinsic scatter will likely be well studied in the future, affecting the analysis of galaxy cluster scaling relations. The presence of intrinsic scatter important to consider as it could be due to selection bias present samples.

5.3 Selection Effects

Selection effects are known to be more apparent within flux limited samples. Effects like the Malmquist and Edington effect have been well studied. Malmquist effects result in the mean luminosity of the sample being increased and will affect the normalisation of the derived L-T relation. This effect is seen within the X-ray sample as higher redshift clusters have above average luminosity. The Eddington effect occurs when clusters on the edge of the flux limit are either scatted over or under the limit. The effect will result in changing the mean luminosity of the sample. The effect on the L-T scaling relations can be minimised by having a larger redshift range. For this reason, the effect of this selection bias has been minimised, but with a slightly raised normalisation. As the SZ clusters will not suffer from similar effects. As previously discussed, when referring to morphology. The SZ cluster suffers from archival bias, the effect this may have on the L-T relation is likely to be minimal and is only due to the increased number of merger systems. This effect is responsible for the variation in the morphology distributions seen in Fig 4. To create a sample to have no archival bias will require a statistically complete sample that is reproducible through simulations.

As briefly discussed in Section 5.2.2, cluster type bias is an effect that is present within X-ray samples. This bias is where there is an overrepresentation of CC within X-ray surveys (Mittal et al. 2011). X-ray instruments have been found to be more effective at detecting CC than NCC (Non-Cold Cores) objects (Eckert et al. 2011). Whether this bias is present within SZ samples is not as well understood. The presence of CCs is expected to increase the SZ signal from a source. The SZ signal (y) is proportional to electron temper-

ature (T_e), $y \propto T_e$. A CC would then be creating a higher S/N ratio for a cluster of the same temperature. Pipino & Pierpaoli (2010) found that there is a clear effect of CC on the SZ signal, with a greater effect on the lowest of the detection limit. This will then have a small effect on the SZ sample used in this study as the range of S/N for the selection criteria is relatively large.

6 CONCLUSION

This work has presented the L-T scaling relation and morphological distribution of two samples. An X-ray selected cluster sample of 18 clusters from the ROSAT PSPC All-sky and 400d surveys and an SZ sample of 17 clusters from the 2500-sqr degree SPT SZ survey observed with Chandra X-ray observatory. The aim of which is to identify any selection effects that arise due to the choice in the sample. Understanding how sample selection can affect galaxy cluster properties is important to use them to probe cosmology. The finding of this work has been summarised below.

- Variation in the axial symmetry of clusters seems to be inaccurate when looking at clusters with a low S/N.
- The morphologies of the two samples do not have a statistically significant difference. There are, however, small differences that are likely due to slight archival bias from early detections of SZ clusters.
- There appears to be no significant difference in the L-T scaling relation parameters between the two samples. There are different selection effects that need to be considered for both SZ and X-ray selected samples.
- As SZ selected clusters have not received as much detailed study compared to X-ray clusters. The effect of there selection effects is not as well understood. There is the potential for a CC bias to exist in SZ sample selected for there S/N ratio.

The work shows that it is necessary to carefully consider selection effects of galaxy cluster samples to ensure a correct interpretation of data. Work is needed to increase sample sizes of SZ samples that are not so limited by archival bias. This will aid to better constrain cluster scaling relations and allow for better testing of cosmological parameters.

REFERENCES

Abell G. O., 1958, ApJS, 3, 211
Andersson K., et al., 2011, ApJ, 738, 48
Arnaud M., Pointecouteau E., Pratt G. W., 2005, A&A, 441, 893
Bengaly C. A. P., Bernui A., Ferreira I. S., Alcaniz J. S., 2017, MNRAS, 466, 2799
Birkinshaw M., 1999, Phys. Rep., 310, 97
Bleem L. E., et al., 2015, ApJS, 216, 27
Bulbul E., et al., 2019, ApJ, 871, 50
Buote D. A., Humphrey P. J., 2012, MNRAS, 421, 1399
Dickey J. M., Lockman F. J., 1990, ARA&A, 28, 215
Eckert D., Molendi S., Paltani S., 2011, A&A, 526, A79
Ettori S., Tozzi P., Borgani S., Rosati P., 2003, Memorie della Societa Astronomica Italiana Supplementi, 3, 180
Feindt U., et al., 2013, A&A, 560, A90
Giodini S., Lovisari L., Pointecouteau E., Ettori S., Reiprich T. H., Hoekstra H., 2013, Space Sci. Rev., 177, 247
Gould A., 1993, ApJ, 412, L55
Ikebe Y., Reiprich T. H., Böhringer H., Tanaka Y., Kitayama T., 2002, A&A, 383, 773
Kaiser N., 1986, MNRAS, 222, 323
Kalus B., Schwarz D. J., Seikel M., Wiegand A., 2013, A&A, 553, A56
Kelly B. C., 2007, ApJ, 665, 1489
Kravtsov A. V., Borgani S., 2012, ARA&A, 50, 353
Limousin M., et al., 2012, A&A, 544, A71
Maughan B. J., Giles P. A., Randall S. W., Jones C., Forman W. R., 2012, MNRAS, 421, 1583
Menanteau F., et al., 2012, ApJ, 748, 7
Migkas K., Reiprich T. H., 2018, A&A, 611, A50
Migkas K., Schellenberger G., Reiprich T. H., Pacaud F., Ramos-Ceja M. E., Lovisari L., 2020, A&A, 636, A15
Mittal R., Hicks A., Reiprich T. H., Jaritz V., 2011, A&A, 532, A133
Nurgaliev D., McDonald M., Benson B. A., Miller E. D., Stubbs C. W., Vikhlinin A., 2013, ApJ, 779, 112
Nurgaliev D., et al., 2017, ApJ, 841, 5
Pipino A., Pierpaoli E., 2010, MNRAS, 404, 1603
Rossetti M., et al., 2016, MNRAS, 457, 4515
Short C. J., Thomas P. A., Young O. E., Pearce F. R., Jenkins A., Muanwong O., 2010, MNRAS, 408, 2213
Sunyaev R. A., 1970, Astrophys. Lett., 7, 19
Sunyaev R. A., Zeldovich Y. B., 1972, Comments on Astrophysics and Space Physics, 4, 173
Vikhlinin A., van Speybroeck L., Markevitch M., Forman W. R., Grego L., 2002, ApJ, 578, L107
Vikhlinin A., Burenin R., Forman W. R., Jones C., Hornstrup A., Murray S. S., Quintana H., 2007, in Böhringer H., Pratt G. W., Finoguenov A., Schuecker P., eds, Heating versus Cooling in Galaxies and Clusters of Galaxies. p. 48 (arXiv:astro-ph/0611438), doi:10.1007/978-3-540-73484-0˙9
Vikhlinin A., et al., 2009, ApJ, 692, 1033
Webb J. K., King J. A., Murphy M. T., Flambaum V. V., Carswell R. F., Bainbridge M. B., 2011, Phys. Rev. Lett., 107, 191101
Zwicky F., 1937, ApJ, 86, 217

Certification of ownership of the copyright in a typescript or manuscript

Project Report/Dissertation presented as part of, and in accordance with, the requirements for the Final Degree of MSci/BSc (delete as applicable) at the University of Bristol, Faculty of Science.

I hereby assert that I own exclusive copyright in the item named below. I give permission to the University of Bristol Library to add this item to its stock and to make it available for consultation in the library, and for inter-library lending for use in another library. It may be copied in full or in part for any bona fide library or research worked, on the understanding that users are made aware of their obligations under copyright legislation, i.e. that no quotation and no information derived from it may be published without the author's prior consent.

Author	Rhys Alfred Shaw
Title	Comparative Study Between Sunyaev-Zel'Dovich and X-ray Selected Galaxy Clusters
Date of submission	06/05/2020

Signed: 

Full name: Rhys Alfred Shaw

Date: 06/05/2020

This project/dissertation is the property of the University of Bristol Library and may only be used with due regard to the rights of the author. Bibliographical references may be noted, but no part may be copied for use or quotation in any published work without the prior permission of the author. In addition, due acknowledgement for any use must be made.